Point-by-Point Dip Coated Long-Period Gratings in Microfibers

Xuan-Yu Zhang, Yong-Sen Yu, Chao Chen, Cong-Cong Zhu, Rui Yang, Zi-Jian Liu, Ju-Fa Liang, Qi-Dai Chen, and Hong-Bo Sun, *Member, IEEE*

***Abstract*— A point-by-point dip coating method has been proposed and demonstrated for fabricating long-period gratings (LPGs) in microfibers. Using a high precision 3D translation stage, the grating structure is formed by periodically immersing the microfiber into a miniature polydimethylsiloxane droplet suspended at the end-tip of the single mode fiber. A 10-period LPG with a grating period of about 143 μm fabricated in the 7.6 μm diameter microfiber demonstrates a resonant dip of 19 dB. Investigations of the strain and temperature response characteristics of the fabricated devices show that the devices have great potential for tunable filter and sensor applications with the merits of flexibility and compactness.**

***Index Terms*— Optical fiber sensor, long-period gratings, dip coating, polydimethylsiloxane.**

I. Introduction

MICRO/NANOFIBERS (MNFs) have attracted enormous attentions in recent years, because they possess the characteristics of large evanescent fields and great configurability, which lead to a strong interaction with the surrounding medium and a good mechanical property of the MNFs. MNFs have been used to fabricate many micro devices, such as fiber interferometers [1], resonators [2], fiber gratings [3], [4] and waveguide couplers [5]. Among them, long-period gratings (LPGs) in microfibers (MFs), which are based on the coupling between the fundamental mode and the high-order modes, are of particular interests. Compared to the conventional LPGs fabricated in single mode fibers (SMFs) [6], [7], photonic crystal fibers [8] and hollow core optical fiber [9], the LPGs in MFs have ultra-compact size, which can play more important roles in photonic integrated systems for fiber communications and optical sensing. So far, the LPGs in MFs have been realized mainly by the methods including femtosecond IR laser surface modifying [10], CO_2 laser tapering and heating [11], [12], and structural LPGs by helically coiling [13]. With these methods, a variety of smart structures of LPGs in MFs have been demonstrated and employed for the sensing applications. These works are however mainly dedicated to the fabrication of LPGs based on silica material. Because polymer materials can be artificially synthesized with various novel characteristics, such as optical and biochemical characteristics, how to introduce the polymer materials to modulate the spectra of the MFs is an interesting issue.

As a widely-used approach to deposit films on the substrates of glasses, plastics and metals, the dip coating method has been used to fabricate many useful and interesting optical devices, such as fiber Fabry–Pérot interferometer [14], polymer solar cells [15], optical filters [16] and microlens arrays [17], which owns the merits of versatility, high fabrication efficiency and the flexibility to control the structures and performances of the fabricated devices. Therefore, it is expected that this approach can be applied to fabricate mode-coupling devices in MNFs, such as the fiber gratings, because of the high fractional evanescent field of the MNFs.

In this letter, the point-by-point (PbP) dip coating method is modified to fabricate novel LPGs in MFs. In this method, after a single coating procedure, a tiny polydimethylsiloxane (PDMS) ellipsoid ring is formed on the MF because of the surface tension and the high viscosity of PDMS. With the help of the high precision 3D translation stage, the grating period and period numbers can be controlled. With only 10 periods, a LPG having a period of 143 μm exhibits a resonant dip of 19 dB in the MF with a diameter of $\sim$7.6 μm. For sensing applications, the fabricated devices present a strain sensitivity of -6.2 pm/$\mu\varepsilon$ and a temperature sensitivity of -30.6 pm/°C. The PbP dip coating method provides a new opportunity for making fiber integrated devices in MNFs and the proposed LPGs reveal the advantages of simple fabrication, low cost and compact size.

II. Experiments

The schematic of the experimental setup for fabricating the LPG is illustrated in Fig. 1(a). First of all, a MF is fabricated by tapering a commercial SMF (SMF-28e, Corning) with the flame brushing technique [10]. The core mode of the un-tapered fiber will be coupled to the fundamental mode of the MF with an efficiency of nearly 100% due to the adiabatic taper transition, and the intermodal coupling can be suppressed [13].

Then the fabricated MF is mounted on the 3D translation stage, and its two SMF pigtails are connected to an

Manuscript received July 23, 2014; revised September 14, 2014; accepted September 15, 2014. Date of publication September 19, 2014; date of current version November 21, 2014. This work was supported by the National Basic Research Program of China (973 Program under Grants 2014CB921302 and 2011CB013003) and by National Natural Science Foundation of China under Grants 91123027, 51335008, and 61235003.

The authors are with the State Key Laboratory on Integrated Optoelectronics, College of Electronic Science and Engineering, Jilin University, Changchun 130012, China (e-mail: yuys@jlu.edu.cn; hbsun@jlu.edu.cn).

Color versions of one or more of the figures in this letter are available online at http://ieeexplore.ieee.org.

Digital Object Identifier 10.1109/LPT.2014.2359546

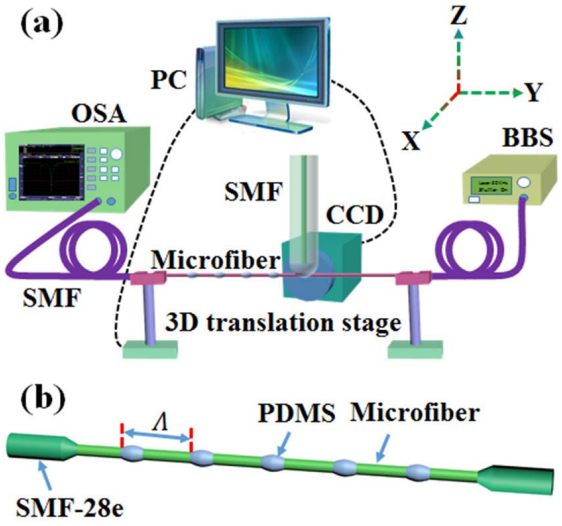

Fig. 1. (a) Schematic of the experimental setup for fabricating the LPGs in MFs with the PbP dip coating method. (b) Schematic diagram of the proposed LPG.

optical spectrum analyzer (OSA) (AQ6370B, Yokogawa) with a wavelength resolution of 0.02 nm and to a supercontinuum broadband light source (BBS) (Superk Compact, NKT Photonics) [18], respectively. Another SMF with a droplet of PDMS (Sylgard 184, Dow corning) at the fiber end-tip, which is formed by dipping the cleaved SMF into the PDMS solution [19] with a fusion splicer (FSU-975, Ericsson), is fixed above the MF with another 3D translation stage. The PDMS solution is prepared with base and curing agents in the ratio of 10:1, which has a refractive index of 1.4028 at 1321 nm and a viscosity of 3.5 pa · s [20]. The distance between the MF and the PDMS coated end-tip of the SMF is ascertained by a charge coupled device (CCD).

With the drive program of the 3D translation stage, the MF can be immersed into the PDMS droplet along the Z axis and then drawn out as illustrated in Fig. 1(a). By this way, a PDMS ellipsoid ring that is much smaller than the droplet on the end face of the SMF is coated on the MF, forming one period of the LPG. Then, the MF is moved along the Y axis with the programmed distance and the above procedure of the MF immersing and drawing out is repeated. During the fabrication process, the transmission spectrum is monitored by the OSA. In this way, the LPG with appropriate grating period and period numbers can be fabricated by the PbP dip coating method. The fabricated LPG is then solidified at the room temperature for two days. However, the cure time could be greatly reduced by putting the proposed LPG in an oven, for example, the cure time would be reduced to about 10 minutes at the temperature of 150 °C [20]. The schematic diagram of the fabricated LPG is presented in Fig. 1(b), consisting of a segment of MF surrounded by the periodical PDMS ellipsoid rings, which has a grating pitch of Λ.

III. Results and Discussions

Fig. 2(a) shows the microscope image of the periodical PDMS ellipsoid rings formed on the MF and Fig. 2(b) presents

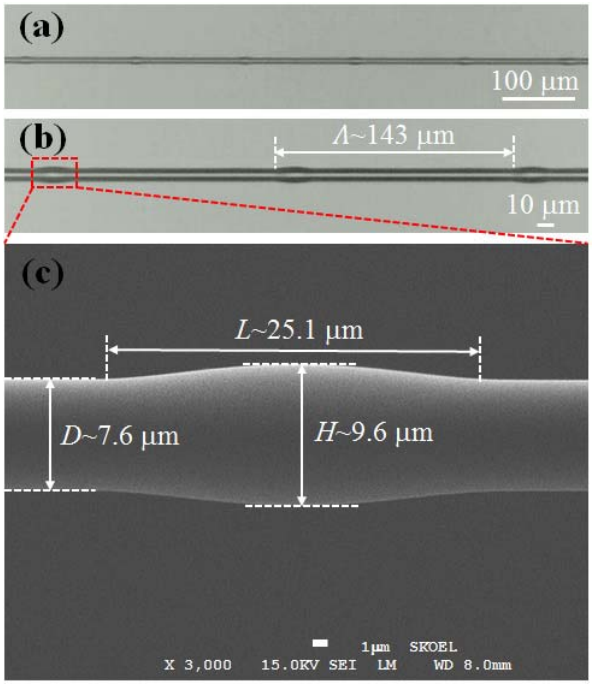

Fig. 2. (a) Microscope image showing the periodical PDMS ellipsoid rings formed on the MF. (b) Further illustration of the fabricated structure. (c) The SEM image of a PDMS ellipsoid ring on the MF.

a further illustration of the fabricated structure, which shows a grating pitch of about 143 μm. The details of an ellipsoid ring formed on the surface of the MF are shown in Fig. 2(c) by the scanning electron microscope (SEM) image, from which it can be seen that the ellipsoid ring has a height of $H \sim 9.6$ μm and a length of $L \sim 25.1$ μm. The average size of the PDMS ellipsoid rings is measured to be 9.2 μm in height and 24.2 μm in length, therefore, the average maximum film thickness is about 0.8 μm that is affected by the so-called capillary number (Ca), which is determined by [21],

$$Ca = \eta V / \gamma \tag{1}$$

where η and γ are the liquid viscosity and surface tension, respectively, and V is the drawing out velocity. The PDMS droplet formed at the end-tip of the SMF normally has a cavity length of about 33 μm, then the volume of the droplet is calculated to be 0.54 nL. On the other hand, the volume of a single PDMS ellipsoid ring formed on the surface of the MF is calculated to be about 0.33 pL, which is thus about 1600 times smaller than that of the PDMS droplet at the end-tip of the SMF, indicating that the PDMS droplet is sufficient to make enough period numbers of the LPG and that the PDMS ellipsoid rings formed on the surface of the MF can have similar shapes when the MF is drawn out of the PDMS droplet. However, because of the difference in the surface tension of the MF, or because of the vibration in the dip coating and the PDMS solidification process, the height and length of the PDMS ellipsoid rings show deviations of ± 0.5 μm and ± 2 μm, respectively.

The evolution of the transmission spectra during the LPG fabricating process is shown in Fig. 3. As can be seen, the

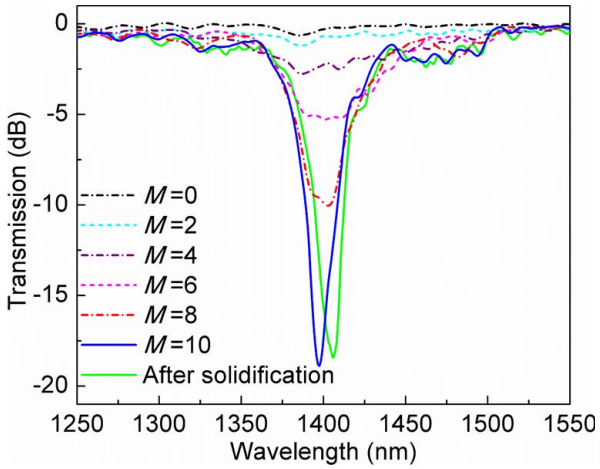

Fig. 3. The evolution of the transmission spectra with the increase of the dip coating numbers and the spectrum after the solidification of the device.

resonant dip grows deeper as the period number M increases. When ten PDMS ellipsoid rings are coated on the surface of the MF, a resonance transmission dip of 19 dB is achieved. After the solidification of the device, the wavelength of the resonant dip shows a red-shift by about 8 nm when compared to the spectrum measured before the solidification, as shown in Fig. 3. This could be due to the change in the morphology or the change in the refractive index of the PDMS ellipsoid rings during the solidification process, both of which would affect the mode coupling. The central wavelength of the resonant dip locates around 1400 nm. After the solidification, the 3 dB bandwidth of the attenuation dip is about 10 nm and the insertion loss of the fabricated device is about 0.8 dB. In addition, it can be found that there are some small dips around the main dip in the transmission spectrum. These small dips may result from the interference between the fundamental mode and high-order modes, in which the excitation of the high-order modes is caused by the dip coated PDMS ellipsoid rings formed on the MF [10], [11]. The modal coupling characteristics of the proposed LPGs can be studied by adopting the two-layer step-index model [11], [22]. This model is investigated in detail in [11], and the investigation covers the mode coupling characteristics in the MFs proposed here. Therefore, no further details in this regard are presented here. According to the calculation, with a diameter of 7.6 μm of the MF and a grating period of 143 μm of the LPG, the HE_{11} mode couples to the HE_{21} mode at a resonant wavelength of around 1400 nm, which agrees with the experiment results.

To investigate the strain sensing characteristics of the proposed LPG, the strain is applied to the LPG by stretching both ends of the MF. As shown in Fig. 4(a), with the increase in the strain applied, the resonant wavelength moves towards the short wavelength because of the photoelastic effect [13], [23], [24]; meanwhile, the intensity of the resonant dip also changes, which might result from the change in the coupling coefficient. The applied strain is in the range of $0-3870\ \mu\varepsilon$. Fig. 4(b) shows the linear fitting of the measured values, which demonstrates a strain sensitivity of -6.2 pm/$\mu\varepsilon$. The strain sensitivity is similar to that of the LPG in MFs

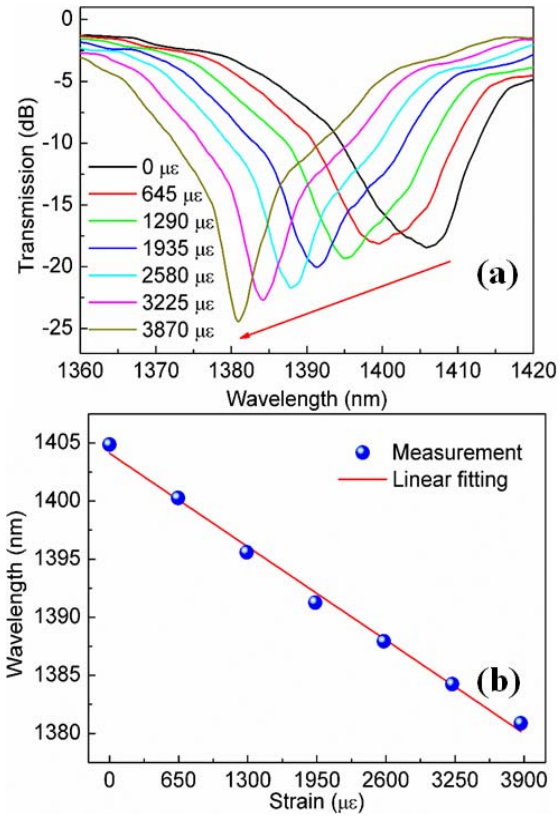

Fig. 4. (a) The evolution of the transmission spectra when the LPG is applied to different strains, the red arrow represents the increase of the strain. (b) Linear fitting of the measurement results.

fabricated by coiling one MF onto another [13]; it is about 14 times larger than that of the conventional LPG [25] and about 2 times larger than that of the nanoimprinted polymer Bragg gratings in MF [26].

By placing a fabricated LPG in a digital oven, we measure the temperature response properties of the LPG. The LPG investigated has a period of about 147 μm and a period number of 12 in the MF with a diameter of about 8.1 μm, which demonstrates a resonant dip at around 1553 nm with an attenuation notch of 21.6 dB. The transmission spectrum of the LPG is shown in Fig. 5, the 3 dB bandwidth of the attenuation dip is about 5 nm and the insertion loss of the device is about 1.4 dB. The LPG is heated in the temperature range of 25 °C–70 °C. As can be seen in the inset of Fig. 5, with the increase of the temperature, the resonant wavelength has a blue-shift [11]. According to the linear fitting of the measurement results, the LPG demonstrates a temperature sensitivity of -30.6 pm/°C, which falls in between the sensitivities of the LPGs in MFs fabricated by femtosecond laser [10] and CO_2 laser [11]. Further, it is about 2 times smaller than that of the LPG fabricated in SMF [27] and about 2 times larger than that of the tilted fiber Bragg gratings in SMF [18].

IV. Conclusions

In conclusion, we have demonstrated the fabrication of the surface corrugated LPGs in MFs by dipping the MFs into the PDMS droplet that is suspended on the end face

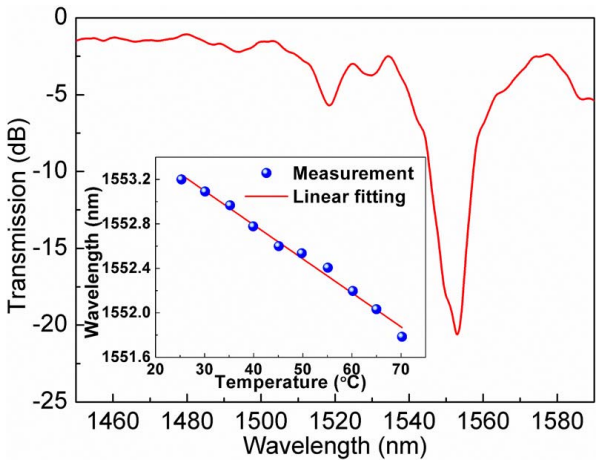

Fig. 5. The transmission spectrum of the LPG fabricated in a 8.1 μm diameter MF with a period of about 147 μm. Inset: the measured wavelength shift with the increase of the temperature and the linear fitting of the measurement results.

of a segment of SMF. This provides a low cost and high efficiency method for fabricating LPGs in MFs. The LPG with a pitch of 143 μm in a MF with the diameter of 7.6 μm shows an attenuation dip at around 1400 nm. The strain and temperature sensing characteristics of the LPGs have also been investigated, which demonstrate the sensitivities of -6.2 pm/$\mu\varepsilon$ and -30.6 pm/°C, respectively. The proposed LPGs may find applications as a tunable band-rejection filter with a large wavelength tuning range and as a strain or temperature sensor based on wavelength shift. Benefiting from the large evanescent fields of the MFs, it would be also possible to realize a gas sensor or biochemical sensor by subsitituting the PDMS with other funtctional polymer materials. Moreover, as the polymer coated on the MF has an ellipsoidal shape and a smooth surface, if the polymer is doped with active materials, each fabricated PDMS ellipsoid ring could be acted as a micro cavity laser to realize lasing.

REFERENCES

[1] J. H. Wo *et al.*, "Refractive index sensor using microfiber-based Mach–Zehnder interferometer," *Opt. Lett.*, vol. 37, no. 1, pp. 67–69, Jan. 2012.

[2] X. S. Jiang, Y. Chen, G. Vienne, and L. M. Tong, "All-fiber add–drop filters based on microfiber knot resonators," *Opt. Lett.*, vol. 32, no. 12, pp. 1710–1712, Jun. 2012.

[3] W. Xiong *et al.*, "Simultaneous additive and subtractive three-dimensional nanofabrication using integrated two-photon polymerization and multiphoton ablation," *Light: Sci. Appl.*, vol. 1, p. e6, Apr. 2012.

[4] W. Luo, J. L. Kou, Y. Chen, F. Xu, and Y. Q. Lu, "Ultra-highly sensitive surface-corrugated microfiber Bragg grating force sensor," *Appl. Phys. Lett.*, vol. 101, no. 13, pp. 133502-1–133502-4, Sep. 2012.

[5] Y. Akihama and K. Hane, "Single and multiple optical switches that use freestanding silicon nanowire waveguide couplers," *Light: Sci. Appl.*, vol. 1, p. e16, May 2012.

[6] Y. Wang, D. N. Wang, M. W. Yang, and C. R. Liao, "Asymmetric microhole-structured long-period fiber gratings," *Sens. Actuators B, Chem.*, vol. 160, no. 1, pp. 822–825, Dec. 2011.

[7] Y. P. Wang, D. N. Wang, W. Jin, Y. J. Rao, and G. D. Peng "Asymmetric long period fiber gratings fabricated by use of CO_2 laser to carve periodic grooves on the optical fiber," *Appl. Phys. Lett.*, vol. 89, no. 15, pp. 151105-1–151105-3, Oct. 2006.

[8] H. R. Chen, K. H. Lin, J. H. Lin, and W. F. Hsieh, "Stress-induced versatile tunable long-period gratings in photonic crystal fibers," *IEEE Photon. Technol. Lett.*, vol. 20, no. 17, pp. 1503–1505, Sep. 1, 2008.

[9] A. Iadicicco, S. Campopiano, and A. Cusano, "Long-period gratings in hollow core fibers by pressure-assisted arc discharge technique," *IEEE Photon. Technol. Lett.*, vol. 23, no. 21, pp. 1567–1569, Nov. 1, 2011.

[10] H. F. Xuan, W. Jin, and S. J. Liu, "Long-period gratings in wavelength-scale microfibers," *Opt. Lett.*, vol. 35, no. 1, pp. 85–87, Jan. 2010.

[11] H. F. Xuan, W. Jin, and M. Zhang, "CO_2 laser induced long period gratings in optical microfibers," *Opt. Express*, vol. 17, no. 24, pp. 21882–21890, Nov. 2009.

[12] G. Kakarantzas, S. G. Leon-Saval, T. A. Birks, and P. St. J. Russell, "Low-loss deposition of solgel-derived silica films on tapered fibers," *Opt. Lett.*, vol. 29, no. 7, pp. 694–696, Apr. 2004.

[13] L. P. Sun, J. Li, L. Jin, and B. O. Guan, "Structural microfiber long-period gratings," *Opt. Express*, vol. 20, no. 16, pp. 18079–18084, Jul. 2012.

[14] Y. T. Tseng, Y. J. Chuang, Y. C. Wu, C. S. Yang, M. C. Wang, and F. G. Tseng, "A gold-nanoparticle-enhanced immune sensor based on fiber optic interferometry," *Nanotechnology*, vol. 19, no. 34, pp. 345501-1–345501-5, Aug. 2008.

[15] Z. Y. Hu, J. J. Zhang, S. Z. Xiong, and Y. Zhao, "Performance of polymer solar cells fabricated by dip coating process," *Sol. Energy Mater. Sol. Cells*, vol. 99, pp. 221–225, Dec. 2011.

[16] H. Köstlin, G. Frank, G. Hebbinghaus, H. Auding, and K. Denissen, "Optical filters on linear halogen-lamps prepared by dip-coating," *J. Non-Cryst. Solids*, vol. 218, pp. 347–353, Sep. 1997.

[17] D. Kang *et al.*, "Shape-controllable microlens arrays via direct transfer of photocurable polymer droplets," *Adv. Mater.*, vol. 24, no. 13, pp. 1709–1715, Apr. 2012.

[18] C. Chao *et al.*, "Reflective optical fiber sensors based on tilted fiber Bragg gratings fabricated with femtosecond laser," *J. Lightw. Technol.*, vol. 31, no. 3, pp. 455–460, Feb. 1, 2013.

[19] X. Y. Zhang *et al.*, "Miniature end-capped fiber sensor for refractive index and temperature measurement," *IEEE Photon. Technol. Lett.*, vol. 26, no. 1, pp. 7–10, Jan. 1, 2014.

[20] *Sylgard 184 Silicone Elastomer Kit, Product Data Sheets*. (Apr. 2014). [Online]. Available: http://www.dowcorning.com/applications/search/default.aspx?R=131EN, accessed Apr. 2, 2014.

[21] D. Quéré, "Fluid coating on a fiber," *Annu. Rev. Fluid Mech.*, vol. 31, no. 1, pp. 347–384, Jan. 1999.

[22] L. M. Tong, J. Y. Lou, and E. Mazur, "Single-mode guiding properties of subwavelength-diameter silica and silicon wire waveguides," *Opt. Express*, vol. 12, no. 6, pp. 1025–1035, Mar. 2004.

[23] C. L. Zhao, L. M. Xiao, J. Ju, M. S. Demokan, and W. Jin, "Strain and temperature characteristics of a long-period grating written in a photonic crystal fiber and its application as a temperature-insensitive strain sensor," *J. Lightw. Technol.*, vol. 26, no. 2, pp. 220–227, Jan. 15, 2008.

[24] R. Yang *et al.*, "S-tapered fiber sensors for highly sensitive measurement of refractive index and axial strain," *J. Lightw. Technol.*, vol. 30, no. 19, pp. 3126–3132, Oct. 1, 2012.

[25] Y. J. Rao, Y. P. Wang, Z. L. Ran, and T. Zhu, "Novel fiber-optic sensors based on long-period fiber gratings written by high-frequency CO_2 laser pulses," *J. Lightw. Technol.*, vol. 21, no. 5, pp. 1320–1327, May 2003.

[26] F. X. Gu, H. K. Yu, W. Fang, and L. M. Tong, "Nanoimprinted polymer micro/nanofiber Bragg gratings for high-sensitivity strain sensing," *IEEE Photon. Technol. Lett.*, vol. 25, no. 1, pp. 22–24, Jan. 1, 2013.

[27] Y. P. Wang, D. N. Wang, and W. Jin, "CO_2 laser-grooved long period fiber grating temperature sensor system based on intensity modulation," *Appl. Opt.*, vol. 45, no. 31, pp. 7966–7970, Nov. 2006.